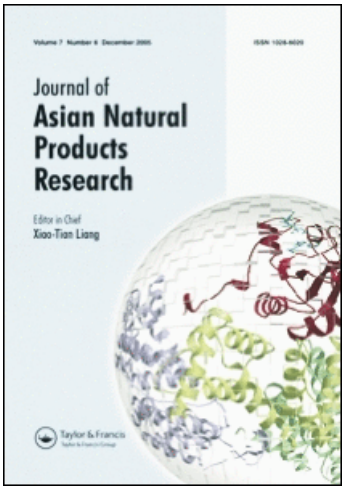

Journal of Asian Natural Products Research
Publication details, including instructions for authors and subscription information:
http://www.informaworld.com/smpp/title~content=t713454007

Flavonoids from *Vitex trifolia* L. inhibit cell cycle progression at G_2/M phase and induce apoptosis in mammalian cancer cells

Wen-Xin Li[ab]; Cheng-Bin Cui[ac]; Bing Cai[a]; Hai-Yan Wang[a]; Xin-Sheng Yao[bd]
[a] Tianjin Institute for Biomedicinal Research (TIBiR), Tianjin, China [b] The School of Traditional Chinese Materia Medica, Shenyang Pharmaceutical University, Shenyang, China [c] §Marine Drug and Food Institute, Ocean University of China, Qingdao, China [d] ¶Traditional Chinese Medicines, & Natural Products Research Center Shenzhen, Shenzhen, China

To cite this Article Li, Wen-Xin , Cui, Cheng-Bin , Cai, Bing , Wang, Hai-Yan and Yao, Xin-Sheng(2005) 'Flavonoids from *Vitex trifolia* L. inhibit cell cycle progression at G_2/M phase and induce apoptosis in mammalian cancer cells', Journal of Asian Natural Products Research, 7: 4, 615 — 626
To link to this Article: DOI: 10.1080/10286020310001625085
URL: http://dx.doi.org/10.1080/10286020310001625085

Journal of Asian Natural Products Research, Vol. 7, No. 4, August 2005, 615–626

Flavonoids from *Vitex trifolia* L. inhibit cell cycle progression at G_2/M phase and induce apoptosis in mammalian cancer cells

WEN-XIN LI†,‡, CHENG-BIN CUI†,§*, BING CAI†, HAI-YAN WANG† and XIN-SHENG YAO‡,¶

†Tianjin Institute for Biomedicinal Research (TIBiR), Tianjin 300384, China
‡The School of Traditional Chinese Materia Medica, Shenyang Pharmaceutical University, Shenyang 110016, China
§Marine Drug and Food Institute, Ocean University of China, Qingdao 266003, China
¶Traditional Chinese Medicines & Natural Products Research Center Shenzhen, Shenzhen 518057, China

(Received 11 July 2003; revised 4 September 2003; in final form 10 September 2003)

Six flavonoids, persicogenin (**1**), artemetin (**2**), luteolin (**3**), penduletin (**4**), vitexicarpin (**5**) and chrysosplenol-D (**6**), have been isolated for the first time as new cell cycle inhibitors from *Vitex trifolia* L., a Chinese folk medicine used to treat cancers, through a bioassay-guided separation procedure. They were identified by spectroscopic methods. The inhibitory effects of **1**–**6** on the proliferation of mammalian cancer cells have been evaluated by the SRB (sulforhodamine B) method and their effects on cell cycle and apoptosis investigated by flow cytometry with the morphological observation under light microscope and by agarose-gel electrophoresis to detect internucleosomal DNA fragmentation. Compounds **1**–**6** inhibited the proliferation of mouse tsFT210 cancer cells with the IC_{50}s ($\mu g\,ml^{-1}$) > 100 (inhibition rate at 100 $\mu g\,ml^{-1}$, 47.9%) for **1**, > 100 (inhibition rate at 100 $\mu g\,ml^{-1}$, 49.6 %) for **2**, 10.7 for **3**, 19.8 for **4**, 0.3 for **5**, and 3.5 for **6**. Flow cytometric investigations for **1**–**6** demonstrated that **1**–**5** mainly inhibited cell cycle at the G_2/M phase in a dose-dependent manner with a weak induction of apoptosis on the tsFT210 cells, while **6** induced mainly apoptosis of the same tsFT210 cells also in a dose-dependent manner together with a weak inhibition of the cell cycle at the G_0/G_1 and G_2/M phases, demonstrating that **1**–**6** exert their anti-proliferative effect on tsFT210 cells through inhibiting cell cycle and inducing apoptosis. In contrast to the cell cycle G_2/M phase inhibitory main effect on tsFT210 cells, **5** induced mainly apoptosis on human myeloid leukemia K562 cells with a weak inhibition of the cell cycle at the G_2/M phase. The present result provides flavonoids **1**–**6** as new cell cycle inhibitors and **1** and **4** as new anticancer flavonoids, which not only provide the first example of cell cycle G_2/M phase inhibitory and apoptosis-inducing constituents of *V. trifolia* L. but also explain the use of *Vitex trifolia* L. by Chinese people to treat cancers.

Keywords: *Vitex trifolia*; Flavonoid; Vitexicarpin; Cell cycle inhibitor; Apoptosis inducer; Anticancer; Verbenaceae

1. Introduction

Fructus Viticis (Manjingzi in Chinese name), a traditional Chinese medicine prepared from the fruit of *Vitex trifolia* L. (family Verbenaceae) [1] is also used as a folk medicine to treat certain

*Corresponding author. Tel.: +86-22-83712588. Fax: +86-22-83712688. E-mail: cuicb@sohu.com

Journal of Asian Natural Products Research
ISSN 1028-6020 print/ISSN 1477-2213 online © 2005 Taylor & Francis Group Ltd
http://www.tandf.co.uk/journals
DOI: 10.1080/10286020310001625085

cancers in parts of China and we have previously reported that the ethanolic extract of the dried fruits of *V. trifolia* L. possesses strong activity in terms of inducing apoptosis and inhibiting cell cycle at the G_0/G_1 and G_2/M phases in mammalian cancer cells [2]. Five labdane-type diterpenes were also reported as the first example of anticancer components responsible for the G_0/G_1 phase inhibitory and partial apoptosis-inducing activities of the title plant [2].

In continuation of that work, we have now isolated six flavonoids, **1**–**6**, from the fruits of *V. trifolia* L. as its bioactive constituents responsible for the cell cycle G_2/M phase inhibitory and partial apoptosis-inducing activities through a bioassay-guided separation procedure.

Flavonoids are well-known plant polyphenolics that are widely distributed in the plant kingdom but methoxylated flavonoids are not distributed far and wide. Also, many flavonoids such as genistein have been known to inhibit cell cycle at the G2/M phase and are used in molecular and cellular biological studies but they are all have free-hydroxy groups on the flavonoidal skeleton. Although **1**–**6** are all known (figure 1), most of them are methoxylated flavonoids, which are rare in plants, and there has been no any report on either their cell cycle inhibitory effect or the anticancer effects for **1** and **4**. The work reported here explores, for the first time, the cell cycle inhibitory properties of **1**–**6** and the anticancer activities for **1** and **4**, covering their isolation, identification and biological properties.

2. Results and discussion

2.1 Isolation and identification of flavonoids 1–6

As we reported previously [2], the crude ethanolic extract (188 g) from the air-dried fruits of *Vitex trifolia* L. has strong activities in terms of inducing apoptosis and inhibiting cell cycle at the G_0/G_1 and G_2/M phases in tsFT210 cells. Because the cell cycle G_0/G_1 phase inhibitory

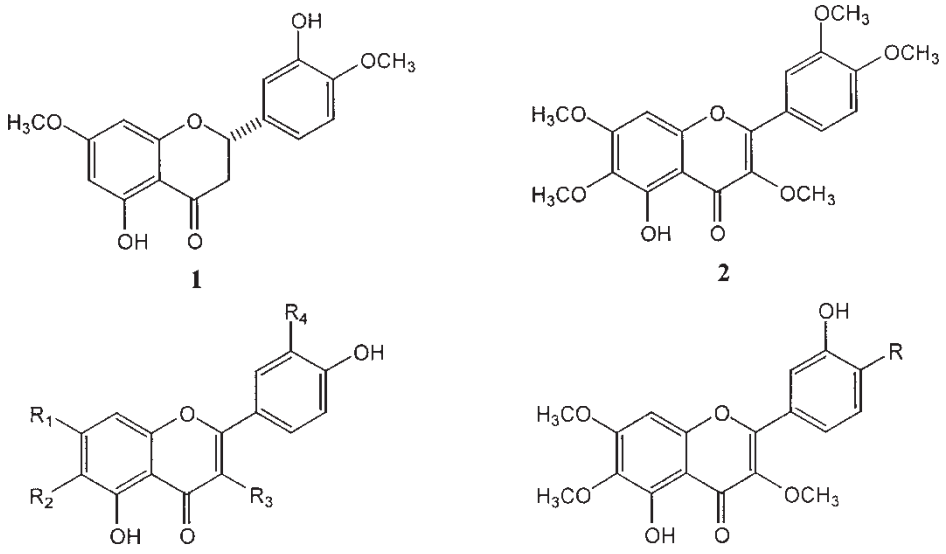

Figure 1. Structures of compounds **1**–**6**.

constituents have been isolated previously [2], the G_2/M phase inhibitory constituents were mainly targeted in the present work and six flavonoidal compounds, **1**–**6**, were isolated as the corresponding bioactive constituents from the crude extracts of *V. trifolia* L. through a bioassay-guided separation procedure.

Compound **1**, yellowish prisms, (MeOH), has a mp of 166.0–167.0°C $C_{17}H_{16}O_6$, $[\alpha]_D^{28}$ −8.33 (*c* 0.4, MeOH), shows a UV maximum absorption typical of the flavanone skeleton at 286.6 nm (log ε 4.13), and was identified as persicogenin according to its FAB-MS, UV, and ^{1}H and ^{13}C NMR data [3].

Compounds **2**–**6** were all obtained as yellow needles and they all gave UV absorption curves typical of a flavonoidal skeleton in MeOH solutions. Eventually they were identified as artemetin (**2**) [4], luteolin (**3**) [5], penduletin (**4**) [6], vitexicarpin (**5**) [7] and chrysosplenol-D (**6**) [7] on the basis of their ESI-MS, UV, and ^{1}H and ^{13}C NMR spectral data.

2.2 Biological activities of 1–6

2.2.1 Flavonoids 1–6 inhibited the proliferation of tsFT210 cells. The inhibitory effect of **1**–**6** on the proliferation of tsFT210 cells was evaluated by the sulforhodamine B (SRB) colorimetric assay [8] (table 1). The inhibition rates (IR%) and the half inhibitory concentration (IC_{50}) values for **1**–**6** were obtained as mean values ± SD (table 1) by three

Table 1. Inhibitory effect of **1**–**6** on the proliferation of tsFT210 cells[a].

Compound	*Concentration* ($\mu g\,ml^{-1}$)	*IR%* ($\overline{X} \pm SD$, $n = 3$)	*IC_{50}* ($\overline{X} \pm SD$, $n = 3$) ($\mu g\,ml^{-1}$)
1	100.0	47.9 ± 0.7	> 100.0
2	100.0	49.6 ± 7.8	> 100.0
3	1.56	12.0 ± 10.7	10.7 ± 5.2
	3.12	24.5 ± 18.7	
	6.25	32.0 ± 19.9	
	12.5	51.9 ± 9.6	
	25.0	63.7 ± 4.2	
	50.0	70.9 ± 3.4	
4	3.12	7.1 ± 19.3	19.8 ± 10.9
	6.25	31.7 ± 3.6	
	12.5	38.4 ± 18.2	
	25.0	54.3 ± 9.9	
	50.0	71.3 ± 7.8	
	100.0	76.6 ± 3.8	
5	0.04	27.4 ± 10.6	0.3 ± 0.1
	0.10	11.3 ± 14.5	
	0.40	57.2 ± 4.6	
	1.0	65.0 ± 3.1	
	4.0	64.3 ± 3.8	
	10.0	66.2 ± 3.0	
6	1.56	29.5 ± 28.8	3.5 ± 2.9
	3.12	49.3 ± 19.5	
	6.25	65.4 ± 10.7	
	12.5	70.9 ± 6.9	
	25.0	64.8 ± 9.6	
	50.0	79.1 ± 6.3	

[a] IC_{50} is the concentration that results in a 50% decrease of viable cell numbers. Data represent mean values of three independent experiments by the SRB method.

independent measurements (Experimental section). As shown in table 1, **1**–**6** all inhibited the proliferation of tsFT210 cells, with that of **5** being the strongest.

2.2.2 Flavonoids 1–5 arrested cell cycle at the G_2/M phase and 6 induced apoptosis in tsFT210 cells. The cell cycle inhibitory and apoptosis-inducing activities were assayed by flow cytometry, accompanied with morphological observations of the cells under a light microscope.

Flavonoids **1**–**5** mainly inhibited the cell cycle progression of tsFT210 cells at the G_2/M phase in a dose-dependent manner although a weak induction of apoptosis was also detected in the tested concentration ranges (table 2). There are significant accumulations of the tsFT210 cells at the G_2/M phase after treatment of the cells with 100, 25, 6.25, 50, and 1.0 μg ml^{-1} of **1**–**5**, respectively, for 17 h (figure 2). At low concentrations of **1**–**5**, however, the numbers of cells

Table 2. Effects of **1**–**6** on cell cycle and apoptosis ($\overline{X}$ ± SD, $n = 3$)[a].

Groups	*Concentrations* (μg ml^{-1})	*Distribution of cells (%)*			
		Apo	*G_0/G_1*	*S*	*G_2/M*
Control	–	1.6 ± 0.7	32.7 ± 4.4	53.1 ± 3.5	14.3 ± 1.0
1	12.5	2.8 ± 1.8	31.4 ± 2.1	53.9 ± 3.6	14.7 ± 4.1
	25.0	3.6 ± 3.0	31.5 ± 1.4	37.1 ± 5.1	30.0 ± 5.5
	50.0	5.6 ± 3.6	21.2 ± 2.6	38.9 ± 6.7	38.0 ± 4.1
	100.0	6.7 ± 4.0	16.9 ± 2.3	23.0 ± 2.9	58.9 ± 3.3
2	3.12	2.4 ± 0.3	37.9 ± 5.3	48.0 ± 1.2	14.0 ± 3.8
	6.25	2.2 ± 0.1	31.5 ± 3.1	49.6 ± 4.1	18.9 ± 5.3
	12.5	3.0 ± 0.8	31.3 ± 1.5	30.3 ± 2.4	38.4 ± 1.2
	25.0[b]	3.1 ± 1.3	31.3 ± 1.7	25.0 ± 0.8	43.7 ± 2.1
3	1.56	2.2 ± 0.1	35.9 ± 5.8	48.4 ± 5.7	15.7 ± 4.8
	3.12	3.7 ± 2.1	32.7 ± 1.6	42.8 ± 6.4	24.6 ± 4.8
	6.25[c]	2.7 ± 1.0	0.5 ± 0.4	30.5 ± 6.3	69.0 ± 6.3
	12.5	4.4 ± 1.4	27.7 ± 7.6	45.6 ± 3.1	26.7 ± 4.5
4	3.12	1.6 ± 0.3	40.1 ± 1.6	47.0 ± 1.4	12.9 ± 3.0
	6.25	2.7 ± 0.7	40.7 ± 7.7	29.6 ± 7.1	29.4 ± 2.1
	12.5	3.6 ± 1.1	39.7 ± 5.0	19.1 ± 5.3	40.9 ± 4.7
	25.0	4.4 ± 0.4	25.0 ± 8.0	26.9 ± 7.9	48.0 ± 0.9
	50.0[c]	4.1 ± 0.1	6.5 ± 3.7	31.7 ± 1.9	62.1 ± 2.3
	100.0	3.1 ± 1.6	23.6 ± 2.3	53.0 ± 1.0	23.3 ± 1.8
5	0.02	2.0 ± 0.2	33.0 ± 0.9	53.2 ± 2.5	13.7 ± 2.5
	0.04	2.5 ± 0.1	30.2 ± 6.8	49.8 ± 6.7	19.7 ± 3.1
	0.06	4.6 ± 0.4	30.8 ± 2.9	43.0 ± 2.5	26.2 ± 2.8
	0.08	5.4 ± 1.2	30.0 ± 0.6	17.7 ± 1.0	52.3 ± 0.5
	0.1	6.3 ± 1.0	19.9 ± 5.0	13.3 ± 5.3	66.8 ± 1.6
	1.0[c]	11.2 ± 3.9	10.3 ± 1.8	1.5 ± 0.6	88.1 ± 1.2
	10.0	12.4 ± 4.7	8.3 ± 4.3	26.2 ± 8.7	65.5 ± 9.8
6	3.12	2.0 ± 0.1	34.9 ± 5.4	49.0 ± 5.5	16.2 ± 2.2
	6.25	4.1 ± 1.4	42.3 ± 3.1	33.1 ± 6.3	24.5 ± 2.6
	12.5	11.7 ± 5.6	43.2 ± 2.7	25.8 ± 2.9	31.0 ± 2.0
	25.0[b]	27.1 ± 1.0	47.4 ± 3.3	23.3 ± 1.7	29.3 ± 4.5

[a] Exponentially growing tsFT210 cells were exposed to **1**–**6** at the concentrations indicated for 17 h and then subjected to flow cytometric analysis after staining of the cell nuclei with propidium iodide. Numbers in the column Apo represent relative percentage of the apoptotic cells counted in the *sub*-G_0/G_1 peak region in total cell numbers. Distribution of the cells within cell cycle (G_0/G_1, S, and G_2/M) was analyzed by the computer software WinCycle (Coulter).

[b] At concentrations > 25 μg ml^{-1}, the sample formed crystals in the tested medium and gave the similar results as that at 25 μg ml^{-1}.

[c] At higher concentrations over that indicated, the sample showed strong cytotoxicity instead of its G_2/M phase inhibitory effect on the cell cycle.

accumulated at the G_2/M phase decreased, accompanied by an increase in the cell populations in the G_0/G_1 and S phases (table 2). Conversely, at concentrations higher than those for G_2/M phase inhibition, **3** and **4** exhibited strong cytotoxicity with no specific effect on the cell cycle, leading to cell numbers obviously less than that of negative control (data not shown).

In contrast, **6** mainly induced apoptosis in the tsFT210 cells with little accumulations of the tsFT210 cells at the G_0/G_1 and G_2/M phases (figure 2), also in a dose-dependent manner (table 2). As shown in figure 2 and table 2, treatment of the tsFT210 cells with **6** at 3.12–25 $\mu g\,ml^{-1}$ for 17 h resulted in a dose-dependent generation of hypodiploid cellular particles due to apoptosis in the *sub*-G_0/G_1 region (Apo both in figure 2 and table 2) together with a small accumulation of the cells at the G_0/G_1 and G_2/M phases. These data indicate that **6** mainly induced apoptosis in the tsFT210 cells, which was confirmed also by morphological observations of the corresponding cells (data not given).

The above results suggested that **1**–**6** inhibit the proliferation of tsFT210 cells through arresting the cell cycle at the G_2/M phase and inducing apoptosis.

2.2.3 Biological effect profile of 5 on tsFT210 and K562 cells. Vitexicarpin (**5**) completely inhibited the cell cycle progression of tsFT210 cells at the G_2/M phase at 1 $\mu g\,ml^{-1}$ (figure 2), which is the same inhibitory efficacy as that of the taxol (1 $\mu g\,ml^{-1}$) used as the positive control. In the dose-dependent experiment (figure 3), the tsFT210 cells treated with **5** were arrested mainly at the G_2/M phase and the proportions of G_2/M phase cells were increased dose-dependently (table 2).

To explore the kinetic effect of **5** on the cell cycle progression of tsFT210 cells, we then performed a time-course experiment with **5** at the concentration of 1.0 $\mu g\,ml^{-1}$ (figure 4).

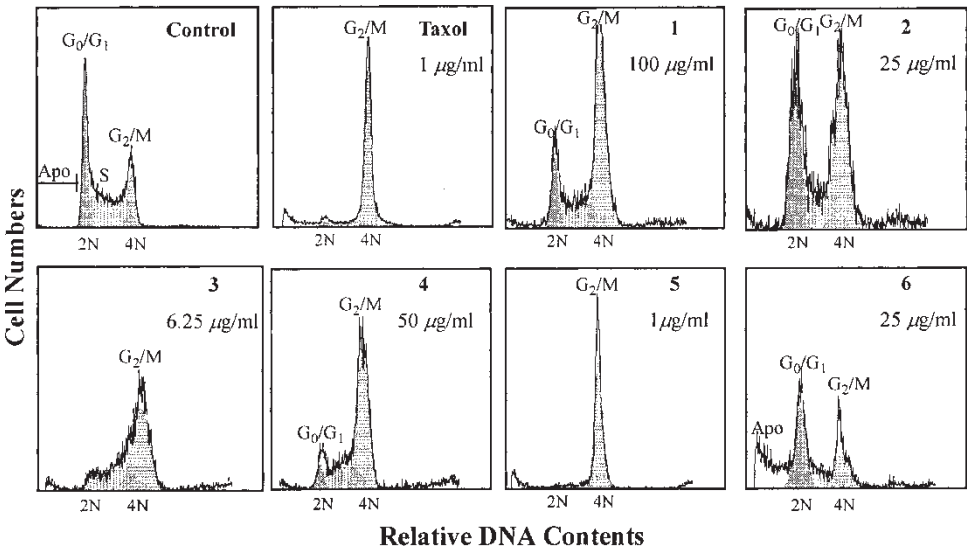

Figure 2. Flow cytometric histograms of tsFT210 cells treated by compounds **1**–**6**. Exponentially growing tsF210 cells were exposed to taxol (positive control) and **1**–**6** respectively at the concentrations indicated; the cell nuclei were stained with propidium iodide and then analyzed by flow cytometry. Open graphs are the raw data from flow cytometry and filled figures indicate the data calculated by the computer software WinCycle (Coulter). The *sub*-G_0/G_1 region indicated as Apo in this figure was defined as the region between the origin of abscissa and the beginning of G_0/G_1 peak, which represents hypodiploid cells due to apoptosis. The result given is a representative of three independent experiments.

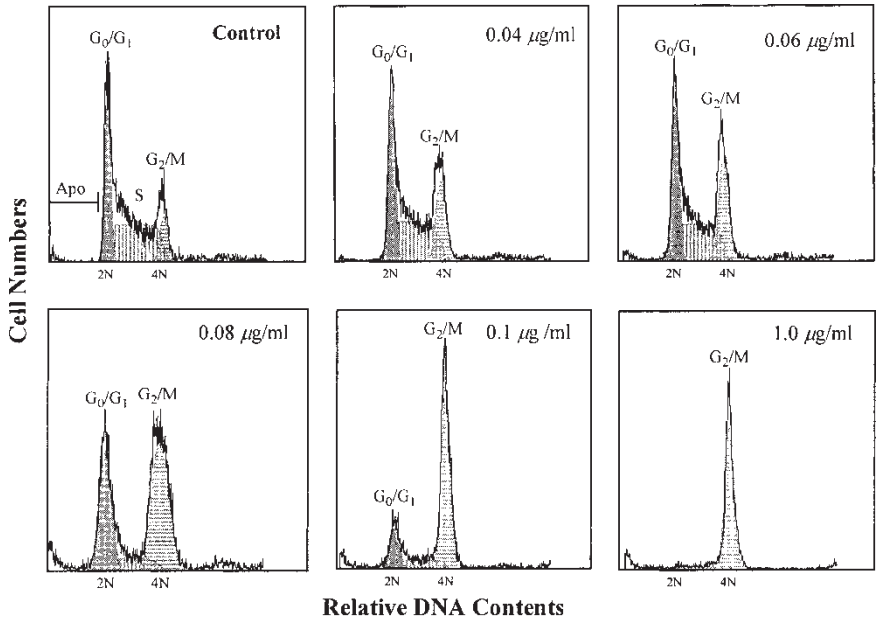

Figure 3. Flow cytometric histograms of tsFT210 cells treated by vitexicarpin (**5**). Exponentially growing tsFT210 cells were treated with **5** at the concentrations indicated for 17 h and then analyzed by flow cytometry after staining of the cell nuclei with propidium iodide. Open graphs are the raw data from flow cytometry and filled figures indicate the data calculated by the computer software WinCycle (Coulter). The *sub*-G_0/G_1 region indicated as Apo is the region between the origin of abscissa and the beginning of G_0/G_1 peak, which represents hypodiploid cells due to apoptosis. The result given is a representative of three independent experiments. The distribution of the cells within cell cycle was analyzed with WinCycle (Coulter) and is summarized in Table II.

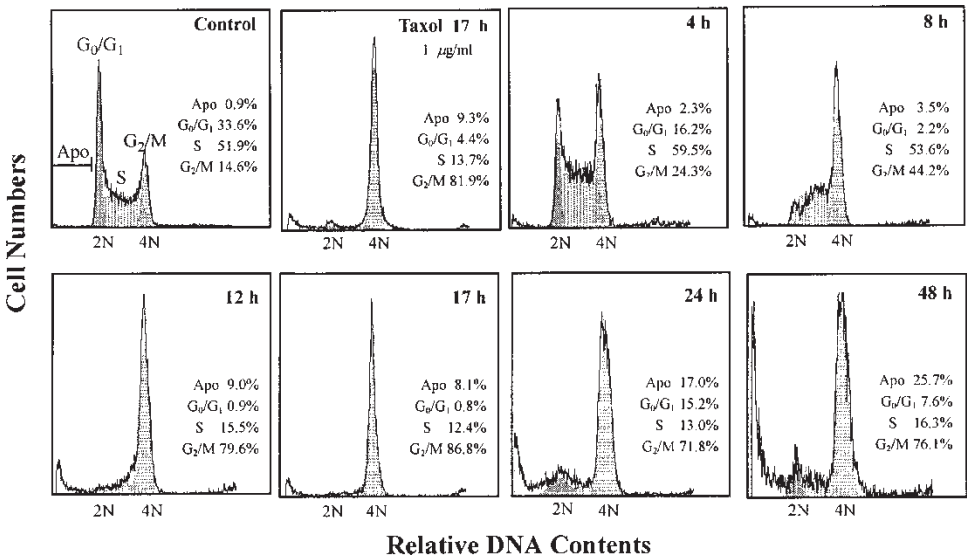

Figure 4. Time course experiment for the effect of **5** on tsFT210 cells. Exponentially growing tsFT210 cells were treated with 1 $\mu g\,ml^{-1}$ **5** for the time periods indicated and analyzed by flow cytometry after staining of the cell nuclei with propidium iodide. The result given is a representative of two independent experiments. Open graphs are the raw data from flow cytometry and filled figures indicate the data calculated by the computer software WinCycle (Coulter). The *sub*-G_0/G_1 region indicated as Apo is the region between the origin of abscissa and the beginning of G_0/G_1 peak, which represents hypodiploid cells due to apoptosis. The distribution of the cells within cell cycle was analyzed with WinCycle (Coulter).

Vitexicarpin (**5**) caused significant inhibition of the cell cycle at the G_2/M phase in the time-dependent accumulations of tsFT210 cells within 4–17 h. However, after 17 h treatment, **5** induced significant apoptosis of the tsFT210 cells in a time-dependent manner, as detected as hypodiploid cellular particles in the *sub*-G_0/G_1 region in the flow cytometric histograms (figure 4). The above result suggests that **5** inhibited at first the cell cycle progression of tsFT210 cells at the G_2/M phase within shorter time periods and then the longer time treatment with **5** resulted in the G_2/M phase cells exiting the cell cycle to undergo apoptosis in a time-dependent manner.

In contrast to the G_2/M phase inhibitory effect on the tsFT210 cells, **5** dramatically induced apoptosis on human myeloid leukemia K562 cells at 1.0 μg ml^{-1} in a time-dependent manner (figure 5). Although the cell cycle progression of K562 cells was arrested at first at the G_2/M phase in the shorter time periods and reached its maximum at 12 h, the G_2/M phase cells exited the cell cycle to undergo apoptosis in turn with the longer time treatments with **5** (figure 5). The morphology of the corresponding K562 cells treated with **5**, observed directly under a light microscope (figure 6), was coincident with the result of flow cytometric analysis: the cells became larger with the treatment times and reached a maximum at 12 h, corresponding to the G_2/M phase arrest detected by flow cytometry (figure 5), and, after 12 h, the cells became metamorphosed to be abnormal (figure 6, 24 h treatment) and eventually showed morphological features typical for apoptosis (figure 6, 48 h treatment).

Apoptosis induced by **5** on K562 cells was also demonstrated by the agarose-gel electrophoresis (figure 7). Internucleosomal DNA fragmentation was detected as clear "DNA

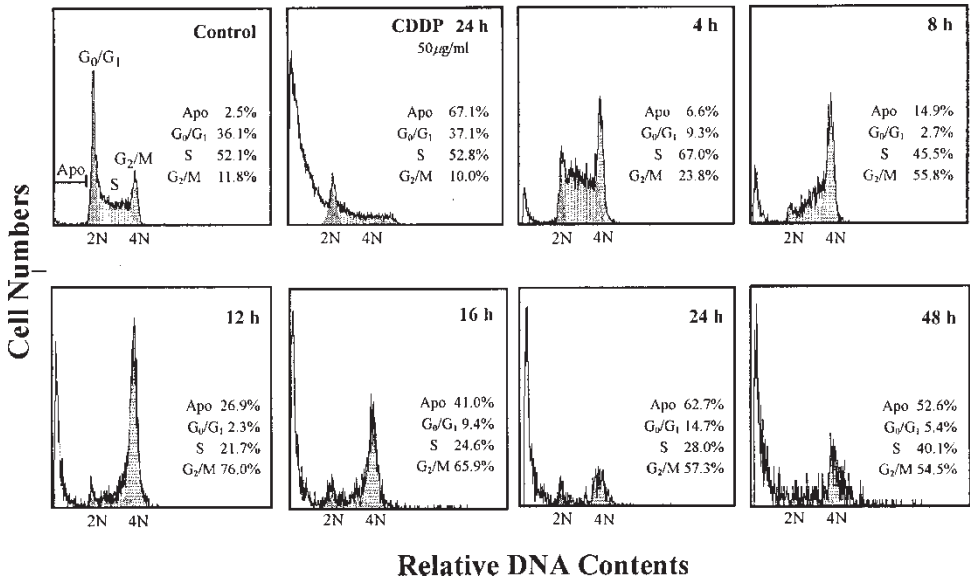

Figure 5. Time course experiment for the effects of **5** on K562 cells. Exponentially growing K562 cells were treated with 1 μg ml^{-1} of **5** for the time periods indicated and then analyzed by flow cytometry after staining of the cell nuclei with propidium iodide. The result given is a representative of two independent experiments. Open graphs are the raw data from flow cytometry and filled figures indicate the data calculated by the computer software WinCycle (Coulter). The *sub*-G_0/G_1 region indicated as Apo is the region between the origin of abscissa and the beginning of G_0/G_1 peak, which represents hypodiploid cells due to apoptosis. The distribution of the cells within cell cycle was analyzed by WinCycle (Coulter).

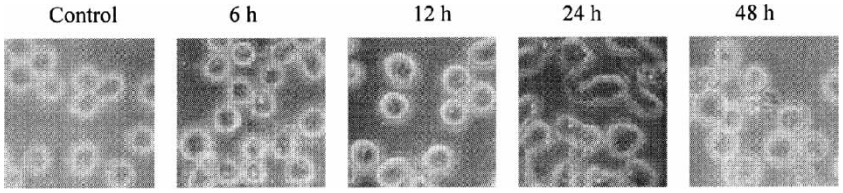

Figure 6. Photographs of K562 cells treated with vitexicarpin (**5**). Exponentially growing K562 cells were treated with 1 μg ml^{-1} of **5** for the time periods indicated and the morphological characteristics of the cells were observed directly and photographed (× 200) under a light microscope.

ladder" from the K562 cells treated with **5** for 24 h, and appeared in a dose-dependent manner (figure 7).

3. Discussions

The results mentioned above demonstrate for the first time that **1**–**6**, especially **5**, are representatives of the cell cycle G_2/M phase inhibitory constituents of *V. trifolia* L. and are responsible, together with the G_0/G_1 phase inhibitory labdane-type diterpenes we reported previously [2], for the cancer chemotherapeutic effect of the title plant, which both explains and provides academic evidence for the use of *V. trifolia* L. by Chinese people to cure certain cancers.

Although flavonoids are well-known plant phenolics with widespread biological activities, including antiproliferative and apoptosis-inducing effects for this class of plant phenolics [9,10], the cell cycle inhibitory effect of **1**–**6** and the anticancer effect of **1** and **4** are described here for the first time. Thus, flavonoids **1**–**6** are new cell cycle inhibitors and **1** and **4** are new members of the anticancer flavonoids. In addition, the antiproliferative and apoptosis-inducing effects of **6** on tsFT210 cells not only confirm the same effects of **6** on HL-60 cells reported by Ko *et al.* [11], but also suggest that the tsFT210 cells treated with **6** underwent apoptosis from S phase of the cell cycle because the dose-dependent generation of apoptotic cellular particles paralleled the decrease of S phase cells (table 2).

During our dose-dependent and time-course experiments with vitexicarpin (**5**), we observed the interesting phenomenon that the K562 cells treated with **5** show characteristic

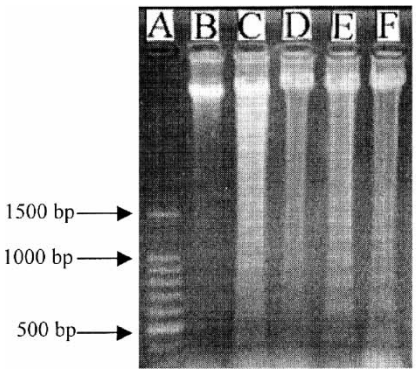

Figure 7. Compound **5** induces DNA ladder in K562 cells detected by agarose gel electrophoresis. DNA was extracted from the K562 cells treated with **5** for 24 h and analysed by 1.5% agarose gel electrophoresis at 40 V: (A) DNA marker, (B) negative control (C) 15.0 μg ml^{-1} CDDP, (D) 0.037 μg ml^{-1} **5**, (E) 0.187 μg ml^{-1} **5**, (F) 0.374 μg ml^{-1} **5**.

metamorphosis; the cells exhibited clavulate morphology at several time periods, as shown in figure 6 for cells treated with **5** at 1 $\mu g\,ml^{-1}$ for 24 h. This phenomenon indicates that **5** acts, probably, on the cytoskeleton, an important target of numerous anticancer drugs [12,13], providing a useful hint to explore its action mechanism. Work on the action mechanism of **5** is being undertaken and will be reported elsewhere.

In conclusion, the present study explores for the first time the cell cycle G_2/M phase inhibitory constituents of *Vitex trifolia* L. and has provided two new anticancer flavonoids, **1** and **4**, together with flavonoids **1**–**6** as new cell cycle inhibitors, suggesting the potential of the flavonoids in chemotherapeutic and/or chemopreventive usage.

4. Experimental

4.1 General experiment procedures

Thin-layer chromatography (TLC) was done on silica gel 60 F254 plates (0.25 mm thick, 20 × 20 cm, Merck), silica gel G plates (0.25 mm thick, 20 × 20 cm, Qingdao Haiyang Chemical Group Co., China) or self-made silica gel 60 F254 (Qingdao Haiyang Chemical Group Co., China) plates (0.25 mm thick, 2.5 × 7.5 cm) and the spots were detected under UV lights (254 and 365 nm) or by the use of 10% aqueous sulfuric acid reagent. Vacuum liquid chromatography and open-column chromatography were carried out on SYNTHWARE™ glass vacuum columns (Tianjin Synthware Glass Instruments Co., Tianjin, China) and glass open columns respectively. Silica gel H (Qingdao Haiyang Chemical group Co., China), Sephadex LH-20 (Pharmacia), reversed silica gel SSC ODS-SS-1020T (Senshu Scientific Co., Ltd., Japan), and polyamide (Taizhou Luqiao biochemical Group Co., China) were used as adsorbents.

Melting points were measured using an XT-type micro melting point apparatus (Beijing Tech Instrument Co. Ltd., China) and are uncorrected. Optical rotations were determined on a JASCO P-1020 polarimeter in MeOH solution and UV spectra were recorded on a Shimadzu UV-2501PC UV-VIS recording spectrophotometer in MeOH solutions. FAB-MS and ESI-MS were measured on an Esquire LC mass spectrometer. ^1H and ^{13}C NMR and 2D NMR spectra were taken on a JEOL Eclips-600 or Bruker AVANCE DRX-500 FT-NMR spectrometer using TMS as internal standard and chemical shifts are recorded as δ values.

4.2 Plant material

The fruits of *V. trifolia* L. (3 kg) were collected in the Chengdu area in Sichuan province, China, in September 1999. The original plant was identified by Professor Q.-S. Sun of Shenyang Pharmaceutical University, China, and a voucher specimen has been deposited at the Herbarium of Shenyang Pharmaceutical University, China.

4.3 Extraction and isolation

Air-dried fruits (3 kg) of *Vitex trifolia* L. were extracted with 95% ethanol (20 l) at room temperature to give a crude extract (188 g) [2]. The whole extract (188 g) was re-extracted in turn with petroleum ether (bp 60–90°C) (2 l), chloroform (2 l) and then EtOAc (1 l) to obtain an active petroleum ether extract (34.2 g), chloroform extract (44.7 g) and then a EtOAc extract (3.65 g), respectively.

The chloroform extract (34.2 g) was subject to vacuum liquid chromatography over silica gel H, using petroleum ether–acetone (PA) and then chloroform–methanol (CM) as eluting solvent, to give six fractions, Fr-1–Fr-6. Of these fractions, Fr-3 (6.28 g, PA 80:20 eluent) was further chromatographed over silica gel H by a stepwise elution with cyclohexane–EtOAc (CE) (1:0 → 0:1) solution to obtain **1** (2 mg) and **2** (53 mg) as yellow prisms, both from MeOH solutions. Fr-4 (5.96 g, CM 95:5 eluent) was separated by Sephadex LH-20 column chromatography with CM (60:40) to obtain **5** (560 mg) and **4** (4.2 mg), both as yellow needles in the order of elution from MeOH solutions. Fr-5 (3.82 g, CM 90:10 eluent) was chromatographed on a Sephadex LH-20 column using CM (60:40) as eluting solvent and **6** (30 mg) was obtained as yellow needles from MeOH solution.

The EtOAc extract (3.65 g) was separated by Sephadex LH-20 and then polyamide--column chromatography to obtain **3** (4.7 mg) as yellow needles from MeOH solution.

4.4 Identification of flavonoids 1–6

4.4.1 Persicogenin. Yellowish needles (MeOH), mp 166–167°C, $C_{17}H_{16}O_6$. FAB-MS *m/z*: 316 $[M]^+$. ^{13}C NMR in CD_3COCD_3 δ (ppm): 198.55 (C-4), 170.04 (C-7), 165.75 (C-5), 165.10 (C-9), 149.89 (C-4′), 148.31 (C-3′), 133.50 (C-1′), 119.51 (C-6′), 115.05 (C-5′), 113.03 (C-2′), 104.57 (C-10), 96.24 (C-6), 95.46 (C-8), 80.93 (C-2), 56.91 (4′-O*C*H_3), 56.77 (7-O*C*H_3), 44.61 (C-3). The above ^{13}C NMR assignments were based on PFG ^1H—^1H COSY, PFG HMQC and PFG HMBC spectroscopy. The UV and ^1H NMR data are identical with those reported for **1** [3].

4.4.2 Artemetin. Yellow needles (MeOH), mp 156–157°C, $C_{20}H_{20}O_8$. ESI-MS *m/z*: 411 $[M + Na]^+$. The UV and ^1H and ^{13}C NMR data are identical with those reported for **2** [4].

4.4.3 Luteolin. Yellow needles (MeOH), mp 326–328°C (dec.), $C_{15}H_{10}O_6$. Negative ESI-MS *m/z*: 285 $[M - H]^-$. The UV and ^1H and ^{13}C NMR data are identical with those reported for **3** [5].

4.4.4 Penduletin. Yellow prisms (MeOH), mp 202–204°C, $C_{18}H_{16}O_7$. ESI-MS *m/z*: 367 $[M + Na]^+$. ^{13}C NMR in $CDCl_3$ δ (ppm): 178.96 (C-4), 158.79 (C-7), 158.13 (C-2), 156.05 (C-4′), 152.70 (C-5), 152.36 (C-9), 138.70 (C-3), 132.27(C-6), 130.76 (C-6′), 129.86 (C-2′), 122.89 (C-1′), 115.85 (C-5′), 115.66 (C-3′), 106.57 (C-10), 90.35 (C-8), 60.91 (6-O*C*H_3), 60.18 (3-O*C*H_3), 56.32 (7-O*C*H_3). The ^{13}C NMR assignments were based on PFG ^1H—^1H COSY, PFG HMQC and PFG HMBC spectroscopy. The UV and ^1H NMR data are identical with those reported for **4** [6].

4.4.5 Vitexicarpin. Yellow needles (MeOH), mp 185–186°C, $C_{19}H_{18}O_8$. ESI-MS *m/z*: 397 $[M + Na]^+$. ^{13}C NMR in $CDCl_3$ δ (ppm): 178.96 (C-4), 158.78 (C-7), 155.62 (C-2), 152.73 (C-5), 152.33 (C-9), 148.75 (C-4′), 145.53 (C-3′), 139.00 (C-3), 132.24 (C-6), 123.61 (C-1′), 121.60 (C-6′), 114.31 (C-5′), 110.37 (C-2′), 106.60 (C-10), 90.32 (C-8), 60.89 (6-O*C*H_3), 60.15 (7-O*C*H_3), 56.32 (3-O*C*H_3), 56.05 (4′-O*C*H_3). The ^{13}C NMR assignments were based on PFG ^1H—^1H COSY, PFG HMQC and PFG HMBC spectroscopy. The UV and ^1H NMR data are identical with those reported for **5** [7].

4.4.6 Chrysosplenol-D. Yellow prisms (MeOH), mp 232–234°C, $C_{18}H_{16}O_8$. ESI-MS *m/z*: 383 $[M + Na]^+$. ^{13}C NMR in DMSO-d_6 δ (ppm): 178.19 (C-4), 158.59 (C-7), 155.94 (C-2), 151.69 (C-5), 151.65 (C-9), 148.80 (C-4′), 145.25 (C-3′), 137.64 (C-3), 131.55 (C-6), 122.72 (C-1′), 120.60 (C-6′), 115.68 (C-5′), 115.52 (C-2′), 105.51 (C-10), 91.24 (C-8), 60.02 (6-O*C*H_3), 59.62 (3-O*C*H_3), 56.44 (7-O*C*H_3). The above ^{13}C NMR assignments were based on PFG ^1H—^1H COSY, PFG HMQC and PFG HMBC spectroscopy. The UV and ^1H NMR data are identical with those for reported **6** [7].

4.5 Cell culture and bioassay

4.5.1 Cell lines and cell culture. A mouse temperature-sensitive $p34^{cdc2}$ mutant, tsFT210, and human myeloid leukemia, K562, cell lines were used for the bioassay. The cells were routinely maintained in RPMI-1640 medium supplemented with 10% FBS under a humidified atmosphere of 5% CO_2 and 95% air. The tsFT210 cells were cultured at 32°C, while the K562 cells were at 37°C.

4.5.2 Cell proliferation assay. The inhibitory effect of flavonoids **1**–**6** on cancer cell proliferation was assayed by the sulforhodamine B (SRB) method, a new colorimetric assay for anticancer-drug screening [8]. SRB is a bright pink aminoxanthene dye with two sulfonic groups. Under mildly acidic conditions, SRB binds to protein basic amino acid residues in trichloroacetic acid (TCA)-fixed cells to provide a sensitive index of cellular protein content that is linear with viable cell density. Thus, SRB can be used to evaluate the anti-proliferative effect of anticancer drugs on cancer cells. Briefly, exponentially growing tsFT210 cells were suspended in fresh medium at the density of 2×10^5 cells ml^{-1}, seeded into 96-well plate and cultured for 24 h under the presence or absence of **1**–**6** at various concentrations. The cells were fixed with 50 μl of 20% TCA solution for 1 h at 4°C, washed 5 times with water and air-dried. Then, 50 μl of SRB solution (0.4 % in 1% acetic acid) was added and stained at room temperature for 30 min. The unbound dye was removed by washing 4 times with 1% acetic acid and then air-dried. To each well, 150 μl of Tris buffer solution (10 mmol l^{-1}, pH 10.5) was added to dissolve the protein-bound dye and the optical density (OD) of each well was determined on a SPECTRA MAX Plus plate reader at 520 nm. Data from triple wells were taken for each concentration of samples on each plate. The inhibition rates (IR%) for compounds **1**–**6** were calculated using mean OD values from $IR\% = (OD_{control} - OD_{sample})/OD_{control} \times 100\%$. Then the concentration required for 50% inhibition of the cell growth, IC_{50}, was determined using the Bliss method. The same experiment was repeated independently three times to obtain the mean IC_{50} and its standard deviation.

4.5.3 Flow cytometry. Flow cytometric analyses for the tsFT210 and K562 cells were carried out according to the method we reported previously [2].

4.5.4 DNA extraction and agarose-gel electrophoresis. Analysis of the internucleosomal DNA fragmentation was performed according to the method of Traganos *et al.* [14]. In brief, the K562 cells treated with **5** were collected by centrifugation, washed twice with ice-cold PBS (pH 7.2) and lysed by suspending overnight at 37°C in a lysis-buffer solution consisted of 100 mmol l^{-1} Tris-HCl buffer (pH 8.5), 5 mmol l^{-1} EDTA, 0.2 mmol l^{-1} sodium chloride, 0.2% (w/v) sodium dodecyl sulfate (SDS) and 200 μl ml^{-1} proteinase K. Then sodium

chloride solution (1.5 mol l^{-1}) was added into the lysate, to give a final sodium chloride concentration of 1 mol l^{-1}, and centrifuged to obtain a supernatant. Ice-cold ethanol was added to the supernatant, to give the final ethanol concentration of 70%, and the resultant solution was kept at -20°C for 2 h to precipitate DNA. The precipitated DNA, collected by centrifugation, was then washed twice with 70% ethanol, air-dried and dissolved by standing at 37°C for 2 h in a TE buffer containing Tris-HCl buffer (10 mmol l^{-1}, pH 8.0), EDTA (10 mmol l^{-1}) and DNase-free RNase A (20 μg ml^{-1}). The DNA sample solution was subjected to electrophoresis at 40 V on a 1.5% agarose gel containing 0.5 μg ml^{-1} EB and photographed with a Polaroid instant pack film T667 under UV light.

Acknowledgements

The authors are grateful to Dr H. Osada, head of the Antibiotics Laboratory, the Institute of Physical and Chemical Research (RIKEN), Japan, for his kind gift of the tsFT210 cell line. This work was supported by the Fund from National Natural Science Foundation of China (C.-B. CUI, No. 39825126), the Fund for the 973-project from the Ministry of Science and Technology (C.-B. CUI, No. 1998051113), China, and the Fund for Cheung Kong Scholar (C.-B. CUI) from the Cheung Kong Scholars Program, Ministry of Education of China. The plant materials were collected and identified by Professor Q.-S. Sun of Shenyang Pharmaceutical University, China.

References

[1] State Pharmacopoeia Commission of China, Pharmacopoeia of P.R.C. pp. 297–298, Chemical Industry Press, Beijing (2000), Part 1.
[2] W.-X. Li, C.-B. Cui, B. Cai, X.-S. Yao. *J. Asian Nat. Prod. Res.*, **7**, 95–105 (2005).
[3] E. Wollenweber, V.H. Dietz, D. Schillo. *Z. Naturforsch., Teil C*, **35**, 685–690 (1980).
[4] A.S. Chawla, A.K. Sharma, S.S. Handa. *Indian J. Chem.*, **30B**, 773–776 (1991).
[5] Y. Kondo, K. Sugiyama, S. Nozoe. *Chem. Pharm. Bull.*, **34**, 4829–4832 (1986).
[6] M. Iinuma, S. Matsuura, K. Kusuda. *Chem. Pharm. Bull.*, **28**, 708–716 (1980).
[7] X.-Y. Zen, Z.-F. Fang, Y.-Z. Wu, H.-D. Zhang. *Chin. J. Mater. Med.*, **21**, 167–168 (1996).
[8] S. Philip, S. Ritsa, S. Dominic, S. Dominic, M. Anne. *J. Natl Cancer Inst.*, **82**, 1107–1112 (1990).
[9] K. Iwashita, M. Kobori, K. Yamaki, T. Tsushida. *Biosci. Biotechnol. Biochem.*, **64**, 1813–1820 (2000).
[10] Y. Rong, E.B. Yang, K. Zhang, P. Mack. *Anticancer Res.*, **20**, 4339–4346 (2000).
[11] W.G. Ko, T.H. Kang, S.J. Lee, N.Y. Kim, Y.C. Kim, D.H. Sohn. *Food Chem. Toxicol.*, **38**, 861–865 (2000).
[12] S.K. Tahir, J.E. Trogadis, J.K. Stevens, A.M. Zimmerman. *Biochem. Cell Biol.*, **70**, 1159–1173 (1992).
[13] S.K. Tahir, E.K. Han, B. Credo, H.-S. Jae, J.A. Pietenpol, C.D. Scatena. *Cancer Res.*, **61**, 5480–5485 (2001).
[14] F. Traganos, J. Kapuscinski, J.P. Gong, A. Barbara, R.J. Darzynkiewicz, Z. Darzynkiewicz. *Cancer Res.*, **53**, 4613–4618 (1993).